Optimization by a genetic algorithm of pyramidal structures made of one, two or three stacks of metal/dielectric layers for a quasi-perfect broadband absorption of UV to near-infrared radiations

Mayer, Alexandre; Griesse-Nascimento, Sarah; Bi, Hai; Mazur, Eric; Lobet, Michael

Published in:
Proceedings of SPIE

DOI:
10.1117/12.2552463

Publication date:
2020

Document Version
Publisher's PDF, also known as Version of record

Optimization by a genetic algorithm of pyramidal structures made of one, two or three stacks of metal/dielectric layers for a quasi-perfect broadband absorption of UV to near-infrared radiations

Mayer, Alexandre, Griesse-Nascimento, Sarah, Bi, Hai, Mazur, Eric, Lobet, Michaël

Alexandre Mayer, Sarah Griesse-Nascimento, Hai Bi, Eric Mazur, Michaël Lobet, "Optimization by a genetic algorithm of pyramidal structures made of one, two or three stacks of metal/dielectric layers for a quasi-perfect broadband absorption of UV to near-infrared radiations," Proc. SPIE 11344, Metamaterials XII, 113441L (1 April 2020); doi: 10.1117/12.2552463

SPIE.

Event: SPIE Photonics Europe, 2020, Online Only, France

Optimization by a genetic algorithm of pyramidal structures made of one, two or three stacks of metal/dielectric layers for a quasi-perfect broadband absorption of UV to near-infrared radiations

Alexandre Mayer[a], Sarah Griesse-Nascimento[b], Hai Bi[b], Eric Mazur[b], and Michaël Lobet[b,c]

[a]Department of Physics, University of Namur, Rue de Bruxelles 61, 5000 Namur, Belgium
[b]John A. Paulson School of Engineering and Applied Sciences, Harvard University, 29 Oxford Street, 02138 Cambridge, MA, USA
[c]Centre Spatial de Liège, Avenue du Pré-Aily, 4031 Angleur, Belgium

ABSTRACT

We use a genetic algorithm to optimize 2-D periodic arrays of truncated square-based pyramids made of successive stacks of metal/dielectric layers. The objective is to achieve a quasi-perfect broadband absorption of normally incident radiations with wavelengths comprised between 420 and 1600 nm. We compare the results one can obtain by considering (i) Ni, Ti, Al or Cr for the metal, and (ii) poly(methyl methacrylate) (PMMA) or TiO_2 for the dielectric. The structures considered consist of only one, two or three stacks of each metal/dielectric combination. The absorption spectrum of these structures is calculated by a Rigorous Coupled Waves Analysis method. A genetic algorithm is then used to determine optimal values for the period of the system, the lateral dimensions of each stack of metal/dielectric and the width of each dielectric. The results show that Ni/PMMA represents the best metal/dielectric combination. With an optimized structure made of only three stacks of Ni/PMMA, it is possible indeed to absorb 99.8% of the considered incident radiations. An integrated absorptance of 99.4% is achieved with three stacks of Ti/PMMA or Cr/PMMA. Aluminium is not to recommend for this application. The solutions obtained with this metal are indeed too sensitive on the geometrical parameters of the system.

Keywords: broadband absorber, nanopyramids, metamaterial, plasmon hybridization, optical engineering, genetic algorithm, optimization

1. INTRODUCTION

Metamaterials make it possible to control and mold the flow of electromagnetic waves in an unprecedented way. They came along with a new paradigm in the manipulation of the refractive index of a material. Negative refraction, superlenses or invisibility cloaks are innovative concepts derived from metamaterials.[1,2] However, metamaterials are mainly made of a combination of dielectric and metallic elements. The latter suffer from high losses in the visible. It opened the way for the development of perfect absorbers that act either at specific wavelengths[3] or over an extended wavelength range.[4–14] Previous work has shown that plasmon hybridization in periodic arrays of truncated square-based pyramids made of 20 stacks of Au/Ge layers leads to an integrated absorptance of 98% of incident light over a 0.2-5.8 μm wavelength range.[15,16] This ultra-broadband absorption is essentially due to (i) an efficient anti-reflection property of these pyramidal structures[17,18] and (ii) a well-designed coupling between the localized surface plasmons found at the metal/dielectric interfaces of each stack.[19–22]

The great performances described in this previous work require the fabrication of a structure that is too demanding in terms of time and resources (20 stacks of metal/dielectric layers are indeed required). There is therefore an interest to determine structures that consist of a reduced number of stacks (only 1, 2 or 3 stacks). In contrast with the approach considered in previous work (stack dimensions varying linearly along the vertical

Further author information: (Send correspondence to A.M.)
A.M.: E-mail: alexandre.mayer@unamur.be, Telephone: +32 81 724720
M.L.: E-mail: mlobet@seas.harvard.edu

Metamaterials XII, edited by Kevin F. MacDonald, Isabelle Staude, Anatoly V. Zayats, Proc. of SPIE
Vol. 11344, 113441L · © 2020 SPIE · CCC code: 0277-786X/20/$21 · doi: 10.1117/12.2552463

axis of the nanopyramids), one can actually give to each stack of metal/dielectric specific and well-tailored dimensions (typically the lateral dimension of each stack and the width of each dielectric layer will be adjustable parameters). This provides the extra degrees of freedom that are necessary to maintain high performances. The physical picture is as follows. The lateral dimensions of the metallic resonators essentially control the plasmonic resonances of the system. The period of the system controls the lateral coupling between these resonances. The widths of the different dielectric layers finally control the vertical coupling between these resonances. A fine tuning between these different parameters makes it possible to achieve the desired broadband absorption. The number of possible parameter combinations to consider grows however exponentially with the number of these parameters. There is therefore a need for efficient global optimization algorithms if we want to adopt this approach.

We showed in previous work that genetic algorithms (GA) are well suited to this type of optical engineering problems.[23–26] The general idea of these algorithms consists in working with a population of individuals that represent possible solutions to the problem. The initial population consists of random individuals. The best individuals are then selected. They generate new individuals for the next generation. Random mutations in the coding of parameters are finally introduced. This strategy is repeated from generation to generation until the population converges, ideally, to the global optimum of the problem.[27–32] For computationally expensive problems, it makes sense to analyze the data collected by the algorithm in order to infer more rapidly the final solution. An approach consists in establishing surrogate models for the function to optimize in order to reduce the number of evaluations.[33–35] Another approach consists in coupling the genetic algorithm with a local optimizer that works on these collected data.[36–38] An idea consists in establishing quadratic approximations of the function to optimize in order to implement this local optimization.[39–46] The algorithm developed in our previous work finally accounts for the experimental resolution of the parameters considered. This resolution sets the accuracy with which each parameter should be determined.

In our previous work on these metamaterial super-absorbers, structures made of one, two or three stacks of nickel/poly(methyl methacrylate) (Ni/PMMA) were considered.[26] Our objective was to achieve a quasi-perfect broadband absorption of normally incident radiations for wavelengths comprised between 420 and 1600 nm (UV to near-infrared). Ni was chosen because it is cheaper and more lossy than Au over the considered wavelength range. PMMA was also chosen as a cheaper alternative to Ge. By tuning the period of the system, the lateral dimensions of each stack of Ni/PMMA and the width of each PMMA layer, an integrated absorptance of 99.8% was achieved with a structure made of only three stacks of Ni/PMMA. The objective of this work is to extend this study by considering all possible combinations between (i) Ni, Ti, Al or Cr for the metal, and (ii) PMMA or TiO_2 for the dielectric. This article is organized as follows. We present in Section 2 the genetic algorithm that is used for the parameter optimization. In Section 3, we use this algorithm to optimize broadband absorbers that consist of one, two or three stacks of the mentioned metal/dielectric materials. Section 4 finally concludes this work.

2. DESCRIPTION OF THE GENETIC ALGORITHM

The genetic algorithm is used to determine the global maximum of an objective function $f = f(x_1, \dots x_n)$, where the n decision variables $x_i \in [x_i^{\min}, x_i^{\max}]$ with a discretization step Δx_i (Δx_i sets the accuracy with which each decision variable should be determined). The decision variables are represented by sequences of binary digits (genes). We use the Gray code to interpret the bit content of these genes.[32,47] The decision variables are hence given by $x_i = x_i^{\min} + \langle \text{gene } i \rangle \times \Delta x_i$, where $\langle \text{gene } i \rangle \in [0, 2^{n_i} - 1]$ refers to the value of the gene. The bit length n_i of each gene is the first integer for which $x_i^{\min} + (2^{n_i} - 1) \times \Delta x_i \geq x_i^{\max}$. $n_{\text{bits}} = \sum_{i=1}^{n} n_i$ refers to the total number of bits in a DNA, i.e. the set of genes used for coding the n decision variables.

We work with a population of n_{pop}=50 individuals. We start with a random population. We evaluate the fitness $f(x_1, \dots x_n)$ of each individual and sort the population from the best individual to the worst. The worst $n_{\text{rand}} = 0.1 \times n_{\text{pop}} \times (1 - p)$ individuals of the population are replaced by random individuals. $p = |s - 0.5|/0.5$ is a progress indicator determined by the genetic similarity s; s corresponds to the fraction of bits in the population whose value is identical to the best individual.[23,47] These random individuals are transferred to the next generation. The remaining $N = n_{\text{pop}} - n_{\text{rand}}$ individuals of the current population participate to the steps of selection, crossover and mutation.

Selection: We select N parents by a rank-based roulette wheel selection, noting that a given individual can be selected several times.[32] *Crossover:* For any pair of parents, we define two children for the next generation either (i) by a one-point crossover of the parents' DNA (probability of 70%), or (ii) by a simple replication of the parents. *Mutation:* The children obtained by crossover are subjected to a modified mutation operator that acts on randomly-shifted Gray codes (see Appendix A of Ref. 26). The idea consists in expressing the genes in randomly-shifted versions of the original Gray code before applying mutations. We then use $m = 0.95/n_{\text{bits}}$ as mutation rate for individual bit flips. The result of these mutations is translated back to the original Gray code (reference encoding used in the rest of the algorithm). The use of randomly-shifted Gray codes when applying mutations helps the genetic algorithm to escape local optima. It also ensures a wider diversity in the displacements generated by these mutations.[26,46]

In order to infer more rapidly the final solution, we apply at each generation a *local optimization* procedure that works on the data collected by the algorithm (see Appendix B of Ref. 26). The idea consists in establishing a quadratic approximation of the fitness in the close neighborhood of the best-so-far individual, by using a singular-value-decomposition technique. Given the quadratic approximation $f(\vec{x}) \simeq a_0 + \vec{A}_1.\vec{X} + \frac{1}{2}\vec{X}.\mathbf{A}_2\vec{X}$ of the fitness, where $\vec{X} = \mathbf{\Delta}^{-1}(\vec{x} - \vec{x}_{\text{ref}})$ with $\vec{x}_{\text{ref}}$ the best-so-far individual and $\mathbf{\Delta} = \text{diag}[\Delta_1, \ldots \Delta_n]/\max_i \Delta_i$ a diagonal matrix that contains appropriate scaling factors, the optimum is given formally by $\vec{x}^* = \vec{x}_{\text{ref}} - \mathbf{\Delta}\mathbf{A}_2^{-1}\vec{A}_1$. We compute the eigensystem $\mathbf{A}_2\vec{x}_k = \lambda_k\vec{x}_k$ of the matrix $\mathbf{A}_2$ in order to express $\vec{x}^* = \vec{x}_{\text{ref}} - \mathbf{\Delta}\sum_k \frac{\vec{x}_k.\vec{A}_1}{\lambda_k}\vec{x}_k$, where the summation is restricted to eigenvalues λ_k for which $|\lambda_k| \geq 10^{-3} \times \lambda_{\max}$ in order to control numerical instabilities ($\lambda_{\max} = \max_k |\lambda_k|$). If the solution obtained by this procedure is within the specified boundaries, it replaces the last individual scheduled for the next generation (a random individual if $n_{\text{rand}} > 0$).

We finally evaluate the fitness f of all individuals scheduled for the next generation. We sort the new population from the best individual to the worst. If the best individual in the new generation is not as good as in the previous generation, the elite of that previous generation replaces an individual chosen at random in the new generation. We repeat these different steps from generation to generation until a termination criterion is met. Since the fitness calculations are computationally expensive, we keep a record with all fitness evaluations in order to avoid any duplication of these evaluations. This record is also used by the local optimization procedure. A multi-agent implementation of this algorithm was developed in order to enable a massive-parallelization of the fitness calculations. We showed in previous work that this algorithm applies with success to typical benchmark problems in 5, 10 and 20 dimensions.[45,46,48]

3. OPTIMIZATION OF PYRAMIDAL STACKS OF METAL/DIELECTRIC LAYERS FOR THE DEVELOPMENT OF QUASI-PERFECT BROADBAND ABSORBERS

Light absorption is a fundamental optical phenomena in which the energy of an electromagnetic wave is transformed in another useful form of energy, such as thermal, chemical or electronic. Applications where light absorption plays an essential role include optical imaging, energy harvesting, local heating or photo-catalysis. Previous work has shown that metamaterials make it possible to develop perfect absorbers that act over an extended wavelength range.[4–14] An approach adopted by Lobet et al. consists in considering periodic arrays of truncated square-based pyramids made of alternating layers of metal/dielectric.[15,16,26] The optimized structure determined by Lobet et al. in 2014 consists of twenty stacks of Au/Ge layers.[15] Each gold layer in this structure has a thickness of 15 nm. This value is smaller than the skin depth over the considered radiation wavelengths. It allows therefore a coupling between the surface plasmons at the two sides of each gold layer. The wavelength associated with these plasmon resonances is proportional to the lateral dimensions of the metallic layers. The dielectric layers play the role of spacer between the metallic resonators. The pyramids stand on a flat 200 nm-thick gold layer. The role of this gold layer is to block the transmission of incident radiations. To maximize the absorptance $A(\lambda) = 1 - T(\lambda) - R(\lambda)$ at any wavelength λ, we need indeed the transmittance $T(\lambda) \to 0$ and the reflectance $R(\lambda) \to 0$. The substrate finally consists of a semi-infinite medium of SiO_2. This metamaterial provides an integrated absorptance of 98.0% over a 0.2-5.8 μm wavelength range.

The ultra-broadband absorption obtained by Lobet et al. in Ref. 15 is essentially due to (i) an efficient anti-reflection property of these pyramidal structures ($R(\lambda) \to 0$)[17,18] and (ii) a well-designed coupling between the

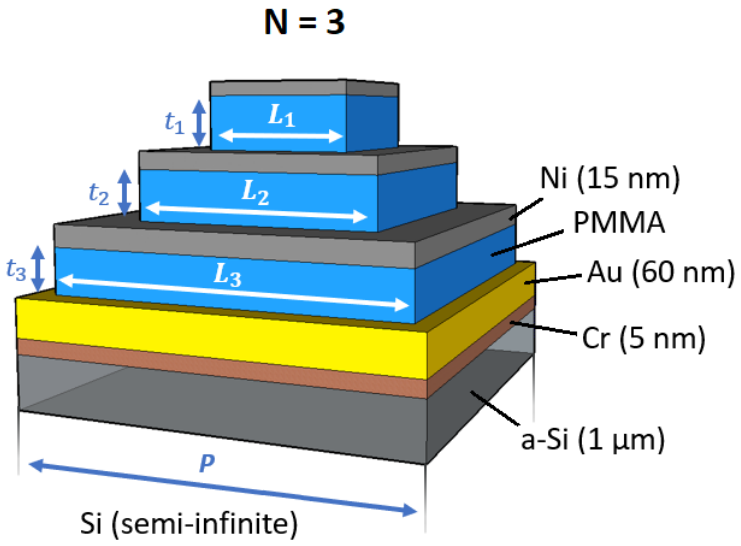

Figure 1. Square-based truncated pyramid made of N=3 stacks of Ni/PMMA layers. The support of the pyramid consists of uniform layers of Au (60 nm), Cr (5 nm) and a-Si (1 micron). We assume an infinite substrate of Si ($\varepsilon = 16$).

localized surface plasmons found at each metal/dielectric interface in these pyramids.[19–22] These controlled plasmonic resonances and their hybridization lead effectively to $A(\lambda) \to 1$. A large number N=20 of metal/dielectric stacks was considered in this previous work. This enables a smooth transition between the refractive index of air and the substrate (anti-reflection effect). The plasmonic resonances of the individual metallic layers also cover a broad wavelength range. It was shown that an hybridization of these plasmon modes occurs. The thickness of the dielectric layers (t_{diel}) was then used to control the vertical coupling between these modes (t_{diel} was given the same value for the N dielectric layers). The period of the system (P) was used to control the lateral coupling between these modes. A manual optimization of N, P and t_{diel} was performed in order to achieve the desired ultra-broadband absorption.

In Ref. 26, Mayer and Lobet used a genetic algorithm to determine broadband absorbers that consist of N=1, 2 or 3 stacks of Ni and PMMA layers (see Fig. 1). The objective was to achieve a quasi-perfect absorption ($A(\lambda) \to 1$) of incident radiations in the wavelength range 420-1600 nm, by tuning the geometrical parameters of these structures. Ni was chosen because it is cheaper and more lossy than Au over the considered wavelength range. PMMA was also taken as cheaper alternative to Ge. The motivation for considering structures made of only 1, 2 or 3 stacks of Ni/PMMA was to limit the study to structures that are compatible with current fabrication scenario. The general strategy for obtaining perfect absorption was similar to the one described in the previous work.[15] The flat support of the pyramids consists of successive uniform layers of Au (60 nm), Cr (5 nm) and amorphous Si (1 micron). A semi-infinite substrate of Si is then considered. The role of the gold layer is again to block the transmission of incident radiations ($T(\lambda) \to 0$). Pyramids are expected to exhibit anti-reflection properties ($R(\lambda) \to 0$). In contrast with the previous study,[15] the dielectric spacers have specific thicknesses t_i, where $i \in [1, N]$. The lateral dimensions L_i of the metallic resonators are also free parameters, except for the constraint that $L_1 < L_2 < L_3 \leq P$. This provides the extra degrees of freedom that are required in order to obtain the desired broadband absorption (despite the reduced number of stacks and thanks to a fine tuning of the plasmon hybridization). By using a genetic algorithm for the parameter optimization, Mayer and Lobet could achieve an integrated absorptance of 99.8% of the considered incident radiations, with a structure that consists of only three stacks of Ni/PMMA.[26]

The objective of this work is to generalize this previous study to a wider variety of materials. We will consider the eight possible combinations between (i) Ni, Ti, Al or Cr for the metal, and (ii) PMMA or TiO_2 for the dielectric. For each metal/dielectric combination, we consider pyramids made of N=1, 2 or 3 stacks of these materials. Each structure is optimized with the genetic algorithm. This extensive study aims at identifying the

best combination of materials in order to achieve a quasi-perfect broadband absorption of incident radiations in the 420-1600 nm wavelength range. The absorptance spectrum of the structures considered is obtained by a Rigorous Coupled Waves Analysis (RCWA) method.[49,50] This method solves Maxwell's equations numerically in laterally periodic systems. We used 11×11 plane waves for the application of the RCWA method and reported values for the refractive indices of each material.[51–54] The figure of merit η of each structure is the integrated absorptance over the considered wavelength range. It is defined by $\eta(\%) = 100 \times \int_{\lambda_{\min}}^{\lambda_{\max}} A(\lambda) d\lambda \,/\, (\lambda_{\max} - \lambda_{\min})$, where $A(\lambda)$ refers to the absorptance of normally incident radiations at the wavelength λ, $\lambda_{\min}$=420 nm and $\lambda_{\max}$=1600 nm. We then use the genetic algorithm to maximize a fitness $f = \eta(P, L_1, t_1, \ldots L_N, t_N)$ given by this figure of merit, by exploring a large number of different parameter combinations for the period P of the system, the lateral dimension L_i of each stack of metal/dielectric and the thickness t_i of each dielectric.

The results provided by the genetic algorithm for the eight material combinations considered are given in Tables 1 and 2. For these different optimizations, the period P of the system could take values between 50 and 500 nm by steps of 1 nm. The lateral dimension L_i of each stack of metal/dielectric could take values between 50 and 500 nm by steps of 1 nm. The thickness t_i of each dielectric could take values between 50 and 250 nm by steps of 1 nm. We use here subscripts i=1, 2 and 3 to refer respectively to the stack at the apex, in the middle or at the bottom of each pyramid. The thickness of each metallic layer was finally fixed to a value of 15 nm. In order to obtain pyramidal structures, we enforced the genetic algorithm to consider only solutions for which $L_1 < L_2 < L_3 \leq P$. When the final solution established by the genetic algorithm was such that $L_3 > P-40$ nm, a second optimization was run by enforcing this time $L_1 < L_2 < L_3$ and $L_3 \leq P - 40$ nm in order to ensure a safe minimal distance of 40 nm between adjacent pyramids. The constrains actually considered for each solution are indicated in the tables. When optimizing structures made of three stacks of metal/dielectric layers, there are actually seven parameters to determine (P, L_1, t_1, L_2, t_2, L_3 and t_3), with a total of 13,936,405,106,594,025 possible parameter combinations. The genetic algorithm is actually able to establish a globally optimal set of parameters after only a few thousands evaluations. This makes the considered optical engineering problem tractable with current super-calculators.

The examination of Tables 1 and 2 reveals that PMMA is a better choice than TiO_2 regarding the dielectric. The use of PMMA leads indeed to higher figures of merit η for all situations considered (i.e., for any choice of metal and for structures made of 1, 2 or 3 stacks). This can be understood by the fact that absorption is higher in TiO_2 than in PMMA. This leads to a slight reduction of the coupling between plasmonic resonances, which in turn reduces the broadband character of the absorption spectrum. Despite this reduction of η, it must be noted that TiO_2 remains a material worth considering for the development of broadband absorbers. An integrated absorptance of 99.3% over the considered 420-1600 nm wavelength range is indeed achieved with only 3 stacks of Ni/TiO_2 (see Table 2).

The best combination of materials is Ni/PMMA (see Table 1). With only 3 stacks of Ni/PMMA, one can indeed achieve an integrated absorptance of 99.8% over the considered 420-1600 nm wavelength range. An integrated absorptance of 99.4% is already achieved with 2 stacks of Ni/PMMA. This material combination is actually that considered in our previous work.[26] Ti/PMMA and Cr/PMMA provide comparable results (η=99.8% for 3 stacks of Ti/PMMA and η=99.7% for 3 stacks of Cr/PMMA). The solutions provided by the genetic algorithm have however $L_3 = P$, which is not appropriate for a realistic device. By enforcing $L_3 \leq P$-40 nm in a second run of the genetic algorithm, we obtain solutions with η=99.4% for 3 stacks of Ti/PMMA or 3 stacks of Cr/PMMA. These solutions are slightly below the integrated absorptance of 99.8% achieved with 3 stacks of Ni/PMMA.

Aluminium is not to recommend for a practical device. The optima found for 1, 2 or 3 stacks of Al/PMMA or Al/TiO_2 turn out indeed to be very sharp ! The solutions obtained with Ni, Ti or Cr are comparatively much broader. This is illustrated in Fig. 2, where we compare maps obtained in the (P, L_1) and (L_1, t_1) planes that pass through the final solution established by the genetic algorithm, when considering either 1 stack of Al/PMMA or 1 stack of Ni/PMMA. These maps are generated by a linear interpolation of the data collected by the genetic algorithm along the optimization. The final solution established by the genetic algorithm is indicated by a star. The black regions in these maps correspond to forbidden solutions (constraint $L_1 \leq P$ not satisfied). These maps show that the solutions obtained with aluminium are indeed very sensitive to deviations of P and

Table 1. Optimal parameters found by the genetic algorithm and figure of merit η for structures made of N=1, 2 or 3 stacks of Ni/PMMA, Ti/PMMA, Al/PMMA or Cr/PMMA (from top to bottom).

Ni / PMMA

	L_1 (nm)	t_1 (nm)	L_2 (nm)	t_2 (nm)	L_3 (nm)	t_3 (nm)	P (nm)	η
N=1 stack $L_1 \leq P$	201	117	-	-	-	-	286	95.0%
N=2 stacks $L_1 < L_2 \leq P$	132	123	227	107	-	-	287	99.4%
N=3 stacks $L_1 < L_2 < L_3$ $L_3 \leq P - 40$ nm	149	131	268	124	369	101	412	99.8%

Ti / PMMA

	L_1 (nm)	t_1 (nm)	L_2 (nm)	t_2 (nm)	L_3 (nm)	t_3 (nm)	P (nm)	η
N=1 stack $L_1 \leq P$	368	134	-	-	-	-	491	89.3%
N=2 stacks $L_1 < L_2 \leq P$	175	117	306	127	-	-	336	98.6%
N=3 stacks $L_1 < L_2 < L_3$ $L_3 \leq P - 40$ nm	161	125	302	126	451	113	491	99.4%

Al / PMMA

	L_1 (nm)	t_1 (nm)	L_2 (nm)	t_2 (nm)	L_3 (nm)	t_3 (nm)	P (nm)	η
N=1 stack $L_1 \leq P$	221	151	-	-	-	-	491	89.2%
N=2 stacks $L_1 < L_2 \leq P$	187	108	263	58	-	-	415	97.9%
N=3 stacks $L_1 < L_2 < L_3 \leq P$	129	112	208	110	294	97	465	98.7%

Cr / PMMA

	L_1 (nm)	t_1 (nm)	L_2 (nm)	t_2 (nm)	L_3 (nm)	t_3 (nm)	P (nm)	η
N=1 stack $L_1 \leq P$	314	124	-	-	-	-	419	88.8%
N=2 stacks $L_1 < L_2 \leq P$	192	121	332	127	-	-	369	98.5%
N=3 stacks $L_1 < L_2 < L_3$ $L_3 \leq P - 40$ nm	151	120	277	127	427	123	467	99.4%

Table 2. Optimal parameters found by the genetic algorithm and figure of merit η for structures made of N=1, 2 or 3 stacks of Ni/TiO_2, Ti/TiO_2, Al/TiO_2 or Cr/TiO_2 (from top to bottom).

Ni / TiO_2

	L_1 (nm)	t_1 (nm)	L_2 (nm)	t_2 (nm)	L_3 (nm)	t_3 (nm)	P (nm)	η
N=1 stack $L_1 \leq P$	186	106	-	-	-	-	265	90.9%
N=2 stacks $L_1 < L_2 \leq P$	196	128	337	82	-	-	388	97.7%
N=3 stacks $L_1 < L_2 < L_3 \leq P$	117	93	189	66	248	72	307	99.3%

Ti / TiO_2

	L_1 (nm)	t_1 (nm)	L_2 (nm)	t_2 (nm)	L_3 (nm)	t_3 (nm)	P (nm)	η
N=1 stack $L_1 \leq P$	354	126	-	-	-	-	500	85.9%
N=2 stacks $L_1 < L_2 \leq P$	194	132	365	89	-	-	403	97.7%
N=3 stacks $L_1 < L_2 < L_3$ $L_3 \leq P - 40$ nm	170	129	339	59	340	50	414	99.1%

Al / TiO_2

	L_1 (nm)	t_1 (nm)	L_2 (nm)	t_2 (nm)	L_3 (nm)	t_3 (nm)	P (nm)	η
N=1 stack $L_1 \leq P$	216	177	-	-	-	-	484	86.9%
N=2 stacks $L_1 < L_2 \leq P$	182	128	343	78	-	-	403	96.5%
N=3 stacks $L_1 < L_2 < L_3 \leq P$	122	112	209	145	312	80	467	98.1%

Cr / TiO_2

	L_1 (nm)	t_1 (nm)	L_2 (nm)	t_2 (nm)	L_3 (nm)	t_3 (nm)	P (nm)	η
N=1 stack $L_1 \leq P$	317	124	-	-	-	-	444	84.9%
N=2 stacks $L_1 < L_2 \leq P$	201	131	368	91	-	-	412	97.5%
N=3 stacks $L_1 < L_2 < L_3$ $L_3 \leq P - 40$ nm	175	127	329	66	353	50	415	98.9%

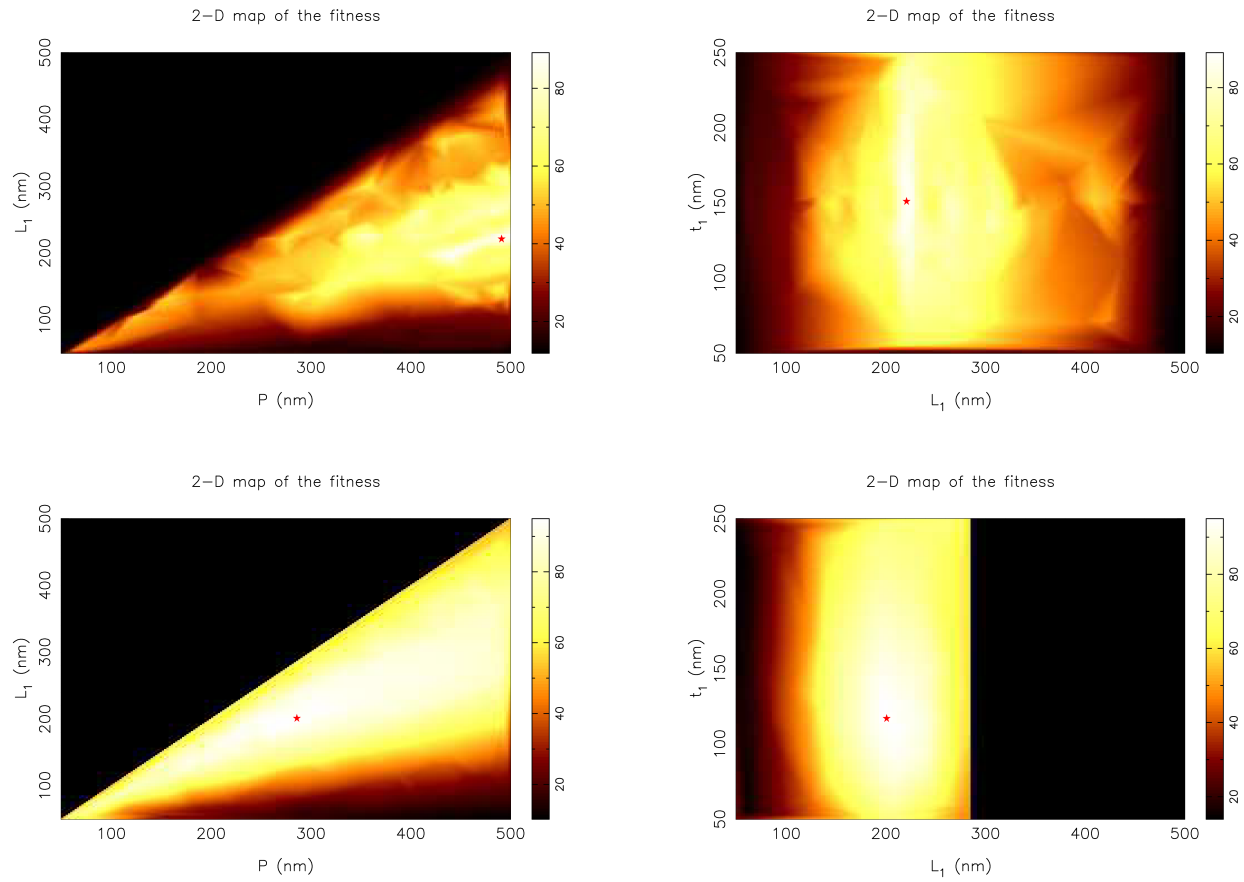

Figure 2. Maps obtained by a linear interpolation of the data collected by the genetic algorithm in the (P, L_1) and (L_1, t_1) planes that pass through the final solution established by the algorithm (indicated by a star). Top: optimization of 1 stack of Al/PMMA (global optimum at P=491 nm, L_1=221 nm and t_1=151 nm). Bottom: optimization of 1 stack of Ni/PMMA (global optimum at P=286 nm, L_1=201 nm and t_1=117 nm).

L_1 from their optimal values, while Ni for example would be more tolerant to these deviations. Aluminium is therefore not recommended for this application.

Figure 3 finally represents the absorptance spectrum obtained with the optimized 3-stack structures given in Tables 1 (PMMA) and 2 (TiO_2). The figures also include for comparison the absorptance obtained with just the flat support of the pyramids (uniform layers of Au (60 nm), Cr (5 nm) and a-Si (1 micron) on a semi-infinite Si substrate). The peak in this last result corresponds to the surface plasmon resonance of the gold layer. The two figures confirm that Ni and PMMA form the best combination of materials. Ti and Cr provide good alternatives. The results obtained with Al confirm that this material should be discarded.

Most solutions in Tables 1 and 2 actually represent good alternatives for the development of broadband absorbers in the 420-1600 nm wavelength range (except for Al as discussed). The best combination of materials is Ni/PMMA, which provides an integrated absorptance of 99.8% with only 3 stacks of metal/dielectric. This design is much easier to fabricate compared to the 20-stack structure considered in the previous work by Lobet et al.[15] Our results are also competitive compared to other devices present in the literature.[4–14] The optimization of structures made of only one or two stacks of metal/dielectric still provides interesting solutions. When considering for example only 2 stacks of Ni/PMMA, one can still absorb 99.4% of the considered incident radiations. An optimized structure made of only 1 stack of Ni/PMMA absorbs 95% of these radiations. These results prove again the interest of an evolutionary approach to optical engineering problems.

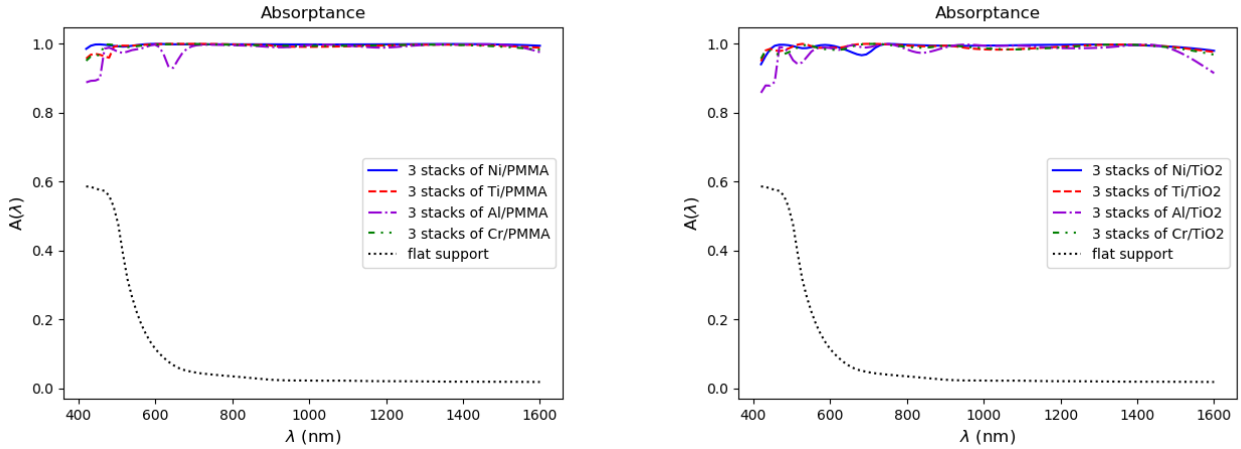

Figure 3. Left: Absorptance $A(\lambda)$ for optimized structures made of 3 stacks of Ni/PMMA (solid), Ti/PMMA (dashed), Al/PMMA (dotdashed) or Cr/PMMA (dotdotdashed). Right: Absorptance $A(\lambda)$ for optimized structures made of 3 stacks of Ni/TiO_2 (solid), Ti/TiO_2 (dashed), Al/TiO_2 (dotdashed) or Cr/TiO_2 (dotdotdashed). The solutions represented in Tables 1 and 2 are those for which $L_3 \leq P$-40 nm. The dotted curves correspond to the absorptance obtained with just the flat support of the pyramids.

4. CONCLUSIONS

We used a genetic algorithm to optimize broadband absorption by periodic arrays of truncated square-based pyramids that consist of 1, 2 or 3 stacks of different metal/dielectric materials. We considered in particular the eight possible combinations between (i) Ni, Ti, Al or Cr for the metal, and (ii) PMMA or TiO_2 for the dielectric. Our objective was to achieve a quasi-perfect broadband absorption of electromagnetic radiations with wavelengths between 420 nm and 1600 nm. A Rigorous Coupled Waves Analysis method was used for the calculation of the absorptance spectra. The genetic algorithm was then used to determine the optimal dimensions of each structure. This study reveals that Ni/PMMA is the best material combination. An optimized structure made of 3 stacks of Ni/PMMA provides indeed an integrated absorptance of 99.8% of the considered radiations. Optimized structures made of three stacks of Ti/PMMA or Cr/PMMA provide an integrated absorptance of 99.4% of these radiations. An integrated absorptance of 99.4% is also achieved with only 2 stacks of Ni/PMMA. The study shows that Al should be discarded for this application because the solutions obtained with this metal are too sensitive on deviations from the optimum. The results obtained with Ni, Ti and Cr are highly competitive. The structures determined in this work have the advantage to be easier to fabricate because of the reduced number of layers involved in the design. Future work will focus on an experimental demonstration of this broadband absorption.

ACKNOWLEDGMENTS

A.M. is funded by the Fund for Scientific Research (F.R.S.-FNRS) of Belgium. He is member of NaXys, Namur Institute for Complex Systems, University of Namur, Belgium. This work was performed while M.L. was a recipient of a Fellowship of the Belgian American Educational Foundation. This research used resources of the "Plateforme Technologique de Calcul Intensif (PTCI)" (http://www.ptci.unamur.be) located at the University of Namur, Belgium, which is supported by the F.R.S.-FNRS under the convention No. 2.5020.11. The PTCI is member of the "Consortium des Equipements de Calcul Intensif (CECI)" (http://www.ceci-hpc.be). The present research also benefited from computational resources made available on the Tier-1 supercomputer of the Fédération Wallonie-Bruxelles, infrastructure funded by the Walloon Region under the grant agreement No. 1117545.

REFERENCES

[1] Pendry, J., "Negative refraction makes a perfect lens," *Phys. Rev. Lett.* **85**(18), 3966–3969 (2000).

[2] Pendry, J. and Smith, D., "Controlling electromagnetic fields," *Science* **312**, 1780–1782 (2006).

[3] Landy, N., Sajuyigbe, S., Mock, J., Smith, D., and Padilla, W., "Perfect metamaterial absorber," *Phys. Rev. Lett.* **100**(20), 207402 (2008).

[4] Hedayati, M., Javaherirahim, M., Mozooni, B., Abdelaziz, R., Tavassolizadeh, A., Chakravadhanula, V., Zaporojtchenko, V., Strunkus, T., Faupel, F., and Elbahri, M., "Design of a perfect black absorber at visible frequencies using plasmonic metamaterials," *Adv. Mater.* **23**(45), 5410–5414 (2011).

[5] Hedayati, M., Faupel, F., and Elbahri, M., "Tunable broadband plasmonic perfect absorber at visible frequency," *Appl. Phys. A-Mater.* **109**(4), 769–773 (2012).

[6] Cui, Y., Fung, K., Xu, J., Yi, J., He, S., and Fang, N., "Exciting multiple plasmonic resonances by a doublelayered metallic nanostructure," *J. Opt. Soc. Am. B* **28**(11), 2827–2832 (2011).

[7] Cui, Y., Fung, K., Xu, J., He, S., and Fang, N., "Multiband plasmonic absorber based on transverse phase resonances," *Opt. Express* **20**(16), 17552–17559 (2012).

[8] Zhu, P. and Guo, L., "High performance broadband absorber in the visible band by engineered dispersion and geometry of a metal-dielectric-metal stack," *Appl. Phys. Lett.* **101**(24), 241116 (2012).

[9] Wang, Y., Sun, T., Paudel, T., Zhang, Y., Ren, Z., and Kempa, K., "Metamaterial-plasmonic absorber structure for high efficiency amorphous silicon solar cells," *Nano Lett.* **12**(1), 440–445 (2012).

[10] Ye, Y., Jin, Y., and He, S., "Omnidirectional, polarization-insensitive and broadband thin absorber in the terahertz regime," *J. Opt. Soc. Am. B* **27**(3), 498 (2010).

[11] Cui, Y., Fung, K., Xu, J., Ma, H., Jin, Y., He, S., and Fang, N., "Ultrabroadband light absorption by a sawtooth anisotropic metamaterial slab," *Nano Lett.* **12**(3), 1443–1447 (2012).

[12] Ding, F., Cui, Y., Ge, X., Jin, Y., and He, S., "Ultra-broadband microwave metamaterial absorber," *Appl. Phys. Lett.* **100**(10), 103506 (2012).

[13] Argyropoulos, C., Le, K., Mattiucci, N., D'Aguanno, G., and Alu, A., "Broadband absorbers and selective emitters based on plasmonic brewster metasurfaces," *Phys. Rev. B* **87**(20), 205112 (2013).

[14] Qiuqun, L., Weixing, Y., Wencai, Z., Taisheng, W., Jingli, Z., Hongsheng, Z., and Shaohua, T., "Numerical study of the meta-nanopyramid array as efficient solar energy absorber," *Opt. Mater. Express* **3**, 1187–1196 (2013).

[15] Lobet, M., Lard, M., Sarrazin, M., Deparis, O., and Henrard, L., "Plasmon hybridization in pyramidal metamaterials: a route towards ultra-broadband absorption," *Opt. Express* **22**(10), 12678–12690 (2014).

[16] Lobet, M. and Henrard, L., "Metamaterials for ultra-broadband super absorbers based on plasmon hybridization," in [*8th International Congress on Advanced Electromagnetic Materials in Microwaves and Optics*], 190–192 (2014).

[17] Clapham, P. and Hutley, M., "Reduction of lens reflexion by the moth eye principle," *Nature* **244**(5414), 281–282 (1973).

[18] Deparis, O., Vigneron, J.-P., Agustsson, O., and Decroupet, D., "Optimization of photonics for corrugated thin-films solar cells," *J. Appl. Phys.* **106**, 094505 (2009).

[19] Prodan, E., Radloff, C., Halas, N., and Nordlander, P., "A hybridization model for the plasmon response of complex nanostructures," *Science* **302**(5644), 419–422 (2003).

[20] Christ, A., Zentgraf, T., Tikhodeev, S., Gippius, N., Kuhl, J., and Giessen, H., "Controlling the interaction between localized and delocalized surface plasmon modes: experiment and numerical calculations," *Phys. Rev. B* **74**(15), 155435 (2006).

[21] Liu, N., Guo, H., Fu, L., Kaiser, S., Schweizer, H., and Giessen, H., "Plasmon hybridization in stacked cut-wire metamaterials," *Adv. Mater.* **19**(21), 3628–3632 (2007).

[22] Pu, M., Feng, Q., Hu, C., and Luo, X., "Perfect absorption of light by coherently induced plasmon hybridization in ultrathin metamaterial film," *Plasmonics* **7**(4), 733–738 (2012).

[23] Mayer, A. and Bay, A., "Optimization by a genetic algorithm of the light-extraction efficiency of a GaN light-emitting diode," *J. Opt.* **17**, 025002 (2015).

[24] Mayer, A., Gaouyat, L., Nicolay, D., Carletti, T., and Deparis, O., "Multi-objective genetic algorithm for the optimization of a flat-plate solar thermal collector," *Optics Express* **22**(S6), A1641–A1649 (2014).

[25] Mayer, A., Muller, J., Herman, A., and Deparis, O., "Optimized absorption of solar radiations in nano-structured thin films of crystalline silicon via a genetic algorithm," *Proc. SPIE* **9546**, 95461N–01–10 (2015).
[26] Mayer, A. and Lobet, M., "UV to near-infrared broadband pyramidal absorbers via a genetic algorithm optimization approach," *Proc. SPIE* **10671**, 1067127–1–11 (2018).
[27] Holland, J., [*Adaptation in Natural and Artificial Systems*], University of Michigan Press, Ann Arbor, Mich. (1975).
[28] De Jong, K., [*An Analysis of the Behaviors of Genetic Adaptative Systems*], PhD thesis, University of Michigan, Ann Arbor, Mich. (1975).
[29] Goldberg, D., [*Genetic Algorithms in Search, Optimization and Machine Learning*], Addison-Wesley, Reading, Mass. (1989).
[30] Hansen, N. and Ostermeier, A., "Completely derandomized self-adaptation in evolution strategies," *Evol. Comput.* **9**(2), 159–195 (2001).
[31] Hansen, N., Muller, S., and Koumoutsakos, P., "Reducing the time complexity of the derandomized evolution strategy with covariance matrix adaptation (cma-es)," *Evol. Comput.* **11**(1), 1–18 (2003).
[32] Eiben, A. and Smith, J., [*Introduction to Evolutionary Computing*], Springer-Verlag, Berlin, second ed. (2007).
[33] Jones, D., "A taxonomy of global optimization methods based on response surfaces," *J. Global Optim.* **21**(4), 345–383 (2001).
[34] Forrester, A., Sobester, A., and Keane, A., [*Engineering Design via Surrogate Modelling: A Practical Guide*], J. Wiley & Sons, Chichester, UK (2008).
[35] Jin, Y., "Surrogate-assisted evolutionary computation: Recent advances and future challenges," *Swarm Evol. Comput.* **1**(2), 61–70 (2011).
[36] Chen, X., Ong, Y.-S., Lim, M.-H., and Tan, K., "A multi-facet survey on memetic computation," *IEEE T. Evolut. Comput.* **15**(5), 591–607 (2011).
[37] Neri, F., Cotta, C., and Moscato, P., [*Handbook of Memetic Algorithms*], Springer, Berlin (2011).
[38] Sapin, E., De Jong, K., and Shehu, A., "A novel ea-based memetic approach for efficiently mapping complex fitness landscapes," in [*Proceedings of the Genetic and Evolutionary Computation Conference*], 85–92 (2016).
[39] Rasheed, K., Ni, X., and Vattam, S., "Comparison of methods for developing dynamic reduced models for design optimization," *Soft Comput.* **9**(1), 29–37 (2005).
[40] Regis, R. and Shoemaker, C., "Local function approximation in evolutionary algorithms for the optimization of costly functions," *IEEE T. Evolut. Comput.* **8**(5), 490–505 (2004).
[41] Paenke, I., Branke, J., and Jin, Y., "Efficient search for robust solutions by means of evolutionary algorithms and fitness approximation," *IEEE T. Evolut. Comput.* **10**(4), 405–420 (2006).
[42] Wanner, E., Guimaraes, F., Takahashi, R., and Fleming, P., "Local search with quadratic approximations into memetic algorithms for optimization with multiple criteria," *Evol. Comput.* **16**(2), 185–224 (2008).
[43] Deep, K. and Das, K., "Quadratic approximation based hybrid genetic algorithm for function optimization," *Appl. Math. Comput.* **203**, 86–98 (2008).
[44] Fonseca, C. and Wanner, E., "A quadratic approximation-based local search operator for handling two equality constraints in continuous optimization problems," in [*IEEE C. Evol. Computat.*], 4911–4917 (2016).
[45] Mayer, A., "A genetic algorithm with randomly shifted gray codes and local optimizations based on quadratic approximations of the fitness," in [*Proceedings of the Genetic and Evolutionary Computation Conference Companion*], 195–196 (2017).
[46] Mayer, A. and Lobet, M., "A genetic algorithm for addressing computationally expensive optimization problems in optical engineering," *Jordan Journal of Physics* **12**(1), 17–36 (2019).
[47] Judson, R., "Genetic algorithms and their use in chemistry," *Reviews in Computational Chemistry* **10**, 1–73 (1997).
[48] Mayer, A., "Genetic algorithms: an evolutionary approach to optical engineering," *Vietnam Journal of Science & Technology* **55**(6A), 9–17 (2017).
[49] Moharam, M. and Gaylord, T., "Rigorous coupled-wave analysis of planar-grating diffraction," *J. Opt. Soc. Am. A* **71**(7), 811–818 (1981).

[50] Lobet, M. and Deparis, O., "Plasmonic device using backscattering of light for enhanced gas and vapour sensing," *Proc. SPIE* **8425**, 842509 (2012).
[51] Johnson, P. and Christy, R., "Optical constants of transition metals: Ti, v, cr, mn, fe, co, ni, and pd," *Phys. Rev. B* **9**(12), 5056–5070 (1974).
[52] Rakic, A., "Algorithm for the determination of intrinsic optical constants of metal films: application to aluminum," *Appl. Optics* **34**(8), 4755 (1995).
[53] Beadie, G., Brindza, M., Flynn, R., Rosenberg, A., and Shirk, J., "Refractive index measurements of poly(methyl methacrylate) (pmma) from 0.4-1.6 μm," *Appl. Optics* **54**(8), 139 (2015).
[54] Siefke, T., Kroker, S., Pfeiffer, K., Puffky, O., Dietrich, K., Franta, D., Ohlidal, I., Szeghalmi, A., Kley, E.-B., and T